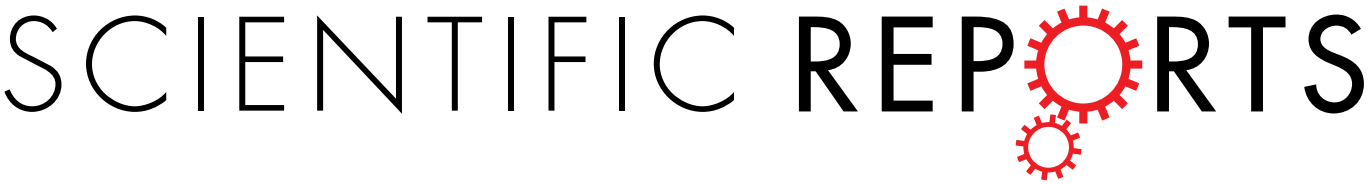

OPEN

Influence of NH_3 plasma and Ti doping on pH-sensitive CeO_2 electrolyte-insulator-semiconductor biosensors

Received: 6 March 2017
Accepted: 13 April 2017
Published online: 25 May 2017

Chyuan-Haur Kao[1,3,4], Che-Wei Chang[1], Yu Tzu Chen[2], Wei Ming Su[2], Chien Cheng Lu[2], Chan-Yu Lin[3] & Hsiang Chen[2]

In this study, CeO_2 pH-sensitive sensing membranes in electrolyte-insulator-semiconductor structures on silicon substrate were fabricated. To enhance sensing performance, the membrane underwent Ti doping and NH_3 plasma treatment on the surface. To examine the effects of Ti doping and plasma treatment, multiple material properties evaluations were conducted using field-emission scanning electron microscopy, X-ray diffraction, atomic force microscopy, and secondary ion mass spectroscopy. Results indicate that Ti doping and plasma treatment can remove defects and enhance crystallization, thereby achieving improved pH-sensing performance of the membrane with high sensitivity, high linearity, low hysteresis voltage and low drift voltage. CeO_2-based EIS membranes with Ti doping and NH_3 plasma treatment show promise for future portable pH-sensitive biosensors.

Within this decade, pH-sensing technologies have been intensively studied for biochemical applications. This is due in large part to the fact that pH value is key to the health of living organisms, influencing function, development and growth of living systems. In the early 20th century, researchers have used colorimetric and electrometric methods to examine the pH values in different solutions by observing their colors and measuring their voltage variations[1]. Since then, light detection and voltage detection have become two distinct methods by which to carry out pH sensing[2]. For pH sensing using the light detection approach, optical fibers were utilized to monitor color changes of the dye in solutions in the 1980s[3]. Recently, Li *et al.* used detection of fluorescent light absorption related to energy level variations to evaluate pH values[4]. Alternately, detection of voltage variation from a semiconductor device began from 1970, when Bergveld invented the first ion-sensitive field effect transistor (ISFET)[5]. An ISFET is derived from a metal oxide semiconductor field effect transistor with an ion-sensing gate structure, in contact with a buffer solution. In the 1990s an electrolyte-insulator-semiconductor (EIS) structure was invented using a sandwiched insulating sensing membrane in contact with an electrolyte on top and a semiconductor on the bottom[6]. EIS biosensing devices have been attracting intensive attention because of their rapid response, robustness, compact size, and possible integration with an on-chip circuit[7,8]. Over the past decade, various types of metal oxides such as Nb_2O_5[9], HfO_2[10], and TiO_2[11] have been used as the sensing insulator in an EIS structure. Recently, some rare earth oxides, with advantages including wide band gaps, large band offsets on Si, and high dielectric constants have been demonstrated as good sensing insulators for EIS biosensing devices[12,13]. Among these rare earth oxides, CeO_2, with a wide bandgap of 3.19 eV and a high dielectric constant, has been used as the sensing material for EIS biosensing devices[14,15]. In addition, Kao *et al.* have proposed the positive effects of annealing on the CeO_2 membrane in 2014[16], and the influence of CF_4 plasma treatment on the CeO_2 sensing insulator in 2015[17]. However, to further improve the material properties of the sensing membrane and hence boost the sensing capability, alternative processes or distinctive treatments are worth exploration and investigation. In addition to the conventional thermal annealing treatment, incorporation of atoms during membrane layering by co-sputtering[18] or the addition of different atoms after membrane deposition with plasma treatment[19] have been

[1]Department of Electronic Engineering, Chang Gung University, Taoyuan, 333, Taiwan, ROC. [2]Department of Applied Materials and Optoelectronic Engineering, National Chi Nan University, Puli, 545, Taiwan, ROC. [3]Kidney Research Center, Department of Nephrology, Chang Gung Memorial Hospital, Chang Gung University, College of Medicine, Taoyuan, Taiwan, ROC. [4]Department of Electronic Engineering, Ming Chi University of Technology, New Taipei City, Taiwan, ROC. Correspondence and requests for materials should be addressed to H.C. (email: hchen@ncnu.edu.tw)

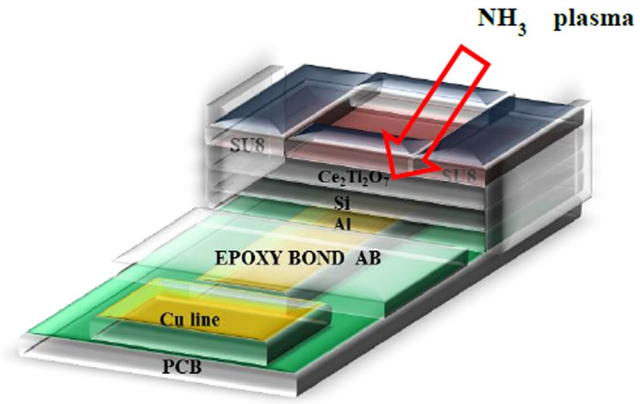

Figure 1. The $Ce_2Ti_2O_7$ EIS structure.

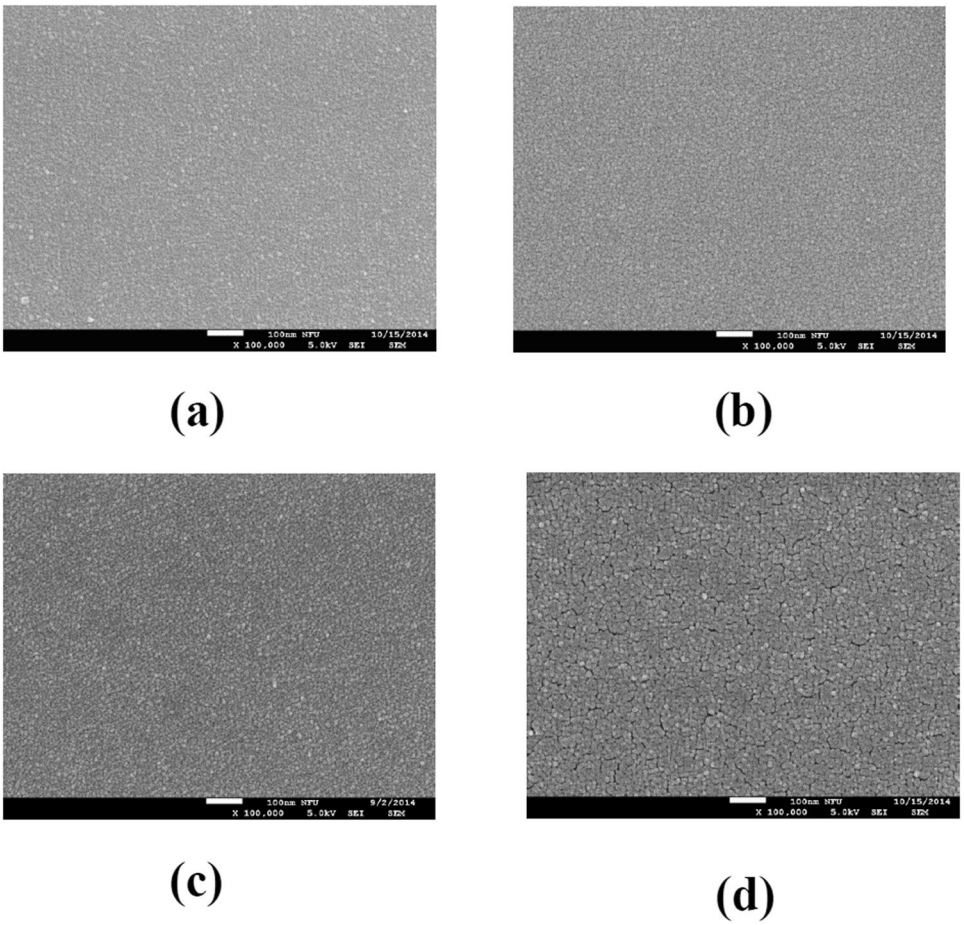

Figure 2. FESEM images of (**a**) the as-deposited CeO_2 sample (**b**) the $Ce_2Ti_2O_7$ sample (**c**) the as-deposited CeO_2 sample with NH3 plasma treatment for 3 min (**d**) the $Ce_2Ti_2O_7$ sample with NH_3 plasma treatment for 3 min.

proposed to reinforce the membrane in order to reducing defects. Recently, the incorporation of Ti atoms[20] and NH_3 plasma treatment[21] have been utilized to improve the sensing membrane performance. Based on the previous report[20], Ti doping in the insulator layer can fix defects in the membrane[22]. Furthermore, addition of N atoms through the NH_3 plasma treatment on the surface of the sensing insulator can mitigate dangling bonds on the membrane surface and hence ameliorate the solution/insulator interface during the sensing operation[23,24]. In this paper, we combined Ti doping and NH_3 plasma treatment to optimize the sensing performance of the membrane.

In this research, CeO_2 membrane-based EIS biosensors were fabricated with Ti doping into the membrane by cosputtering and N-atom incorporation by NH_3 plasma treatment on the surface of the membrane. Moreover, multiple material analyses, including secondary ion mass spectroscopy (SIMS), field-emission scanning electron

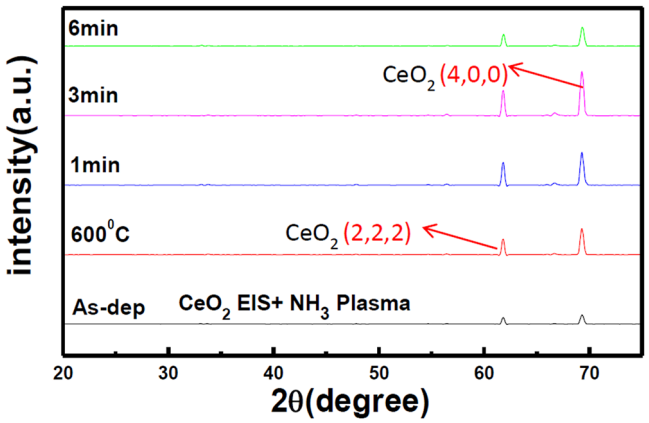

Figure 3. XRD of (**a**) CeO_2 samples with NH3 plasma treatment in various conditions. (**b**) $Ce_2Ti_2O_7$ samples with NH3 plasma treatment for 3 min.

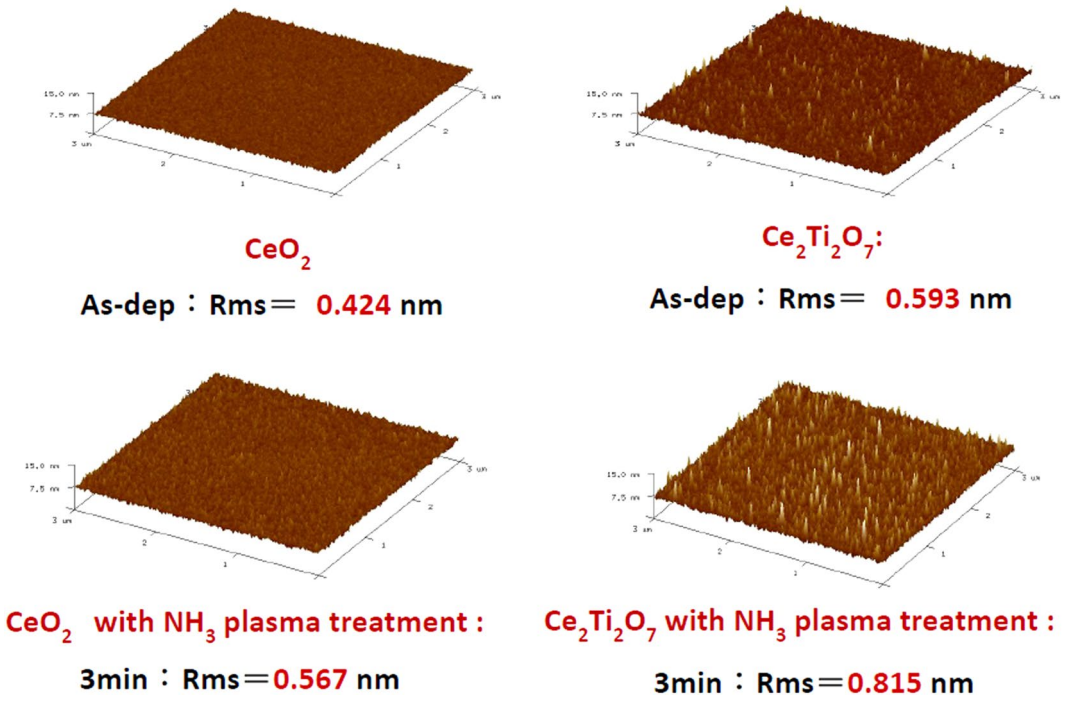

Figure 4. AFM images of the CeO_2 sample without NH_3 plasma treatment and with NH_3 plasma treatment for 3 min. The normalized C-V curve of the $Ce_2Ti_2O_7$ sample without and with NH_3 plasma treatment for 3 min.

microscopy (FESEM), X-ray diffraction (XRD), and atomic force microscopy (AFM) were performed to study the improvements of material properties caused by Ti doping and NH_3 plasma treatment. SIMS results show that the piling up of N atoms may fix interfacial dangling bonds. Moreover, FESEM images clearly indicate that both Ti doping and NH_3 plasma treatment can enhance granization. Consistent with the FESEM images and XRD analysis, AFM images reveal that incorporation of Ti atoms can reinforce the crystallization of the CeO_2 insulator. In addition, the pH-sensing sensing capabilities were measured[25,26]. In line with the material analysis, results indicate that incorporation of Ti doping and NH_3 plasma treatments could effectively improve pH sensing behavior and sensing capability. The Ti-doped NH_3 plasma treated EIS biosensors have the potential to develop future portable biochemical sensors at an industrial level.

Results and Discussion

The detailed EIS structure is illustrated in Fig. 1. Material analyses were performed on the membrane film and sensing measurements were conducted on the EIS sensors. To characterize the influence of Ti addition and NH_3 plasma treatment on the CeO_2 membrane, multiple material characterizations including FESEM, XRD, AFM, and SIMS were performed on CeO_2 and $Ce_2Ti_2O_7$ films with and without NH_3 plasma treatment. First, we used FESEM to view the surface morphologies of CeO_2 and $Ce_2Ti_2O_7$ films as shown in Fig. 2(a,b,c and d). An FESEM

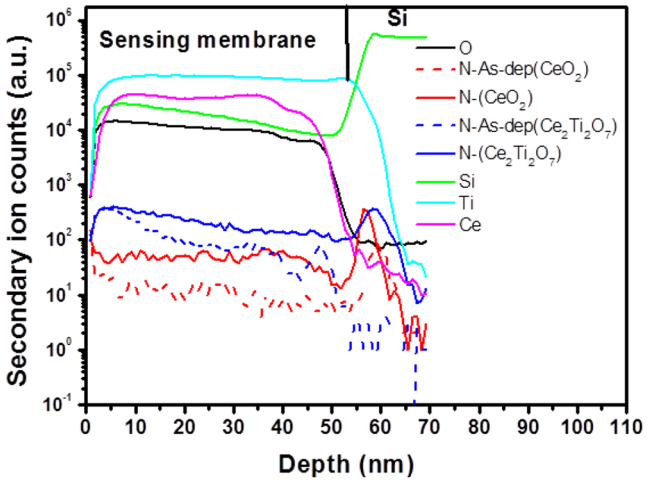

Figure 5. SIMS profiles of CeO_2 or $Ce_2Ti_2O_7$ sensing membrane/Si with NH_3 plasma treatment.

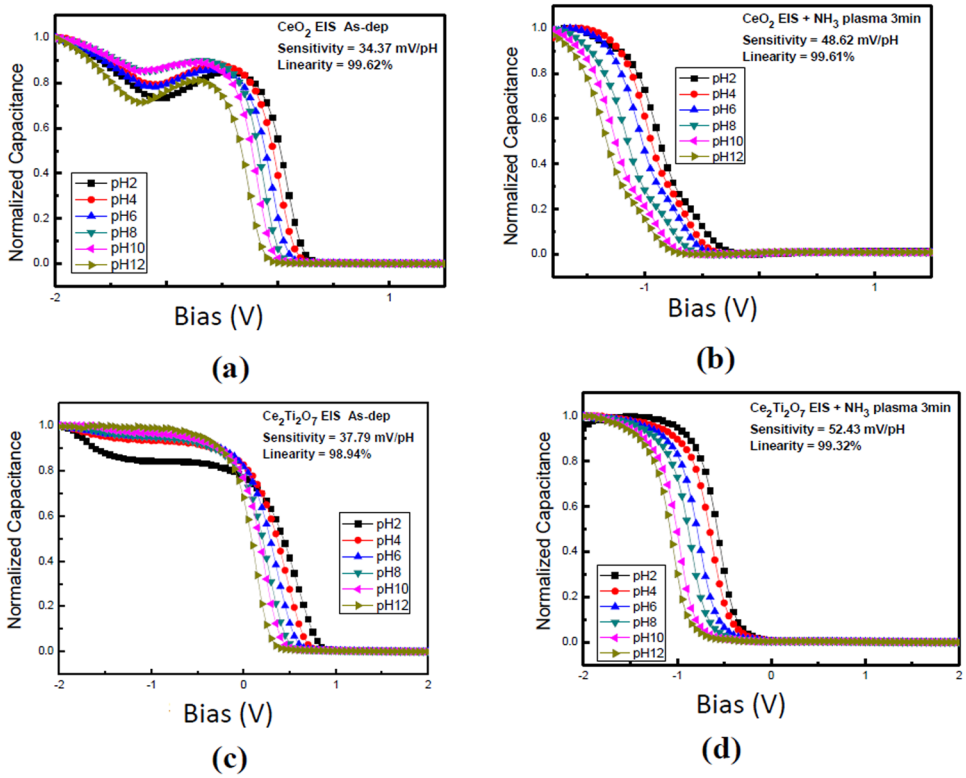

Figure 6. The normalized C-V curve of the CeO_2 sample (**a**) without NH_3 plasma treatment and (**b**) with NH_3 plasma treatment for 3 min. The normalized C-V curve of the $Ce_2Ti_2O_7$ sample (**c**) without and (**d**) with NH_3 plasma treatment for 3 min.

image of the as-deposited CeO_2 film is shown in Fig. 2(a). Compared with the as-deposited CeO_2 film, the FESEM image of the Ti-doped CeO_2 film without NH_3 plasma treatment as shown in Fig. 2(b) reveals that clearer nano-grains could be observed, indicating that Ti addition might reinforce crystallization. Similarly, the CeO_2 film treated with NH_3 plasma as shown in Fig. 2(c) exhibited clearer grain images than the CeO_2 as-deposited film, showing that NH_3 plasma treatment could enhance crystallization as well. Furthermore, CeO_2 film incorporating Ti atoms with NH_3 plasma treatment as shown in Fig. 2(d) exhibited the strongest crystallization among all the samples. In addition, slight cracks around the grains might further enhance the contact area in the membrane/electrolyte surface and boost the sensing performance.

Additionally, we used XRD to examine the CeO_2 films and the $Ce_2Ti_2O_7$ films incorporated with Ti atoms in various NH_3 plasma treatment conditions, as shown in Fig. 3(a and b). Consistent with the FESEM images as

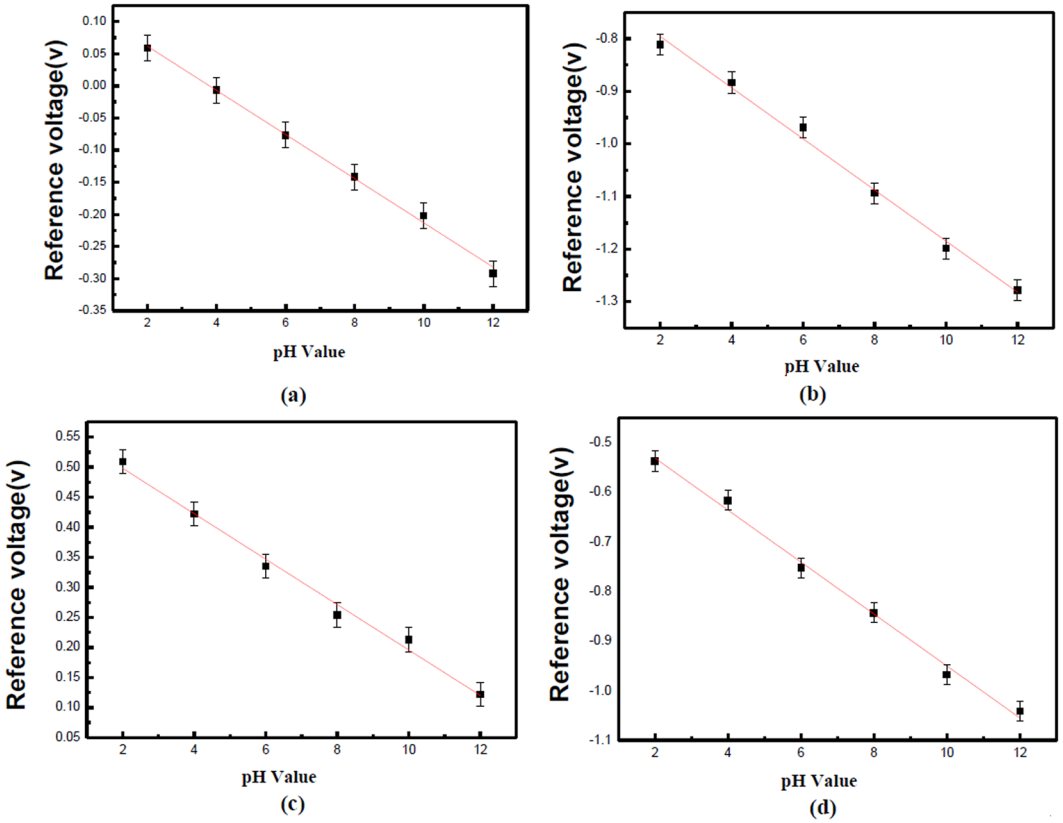

Figure 7. The linearity and sensitivity extracted from normalized C-V curve for the CeO_2 sample (**a**) without NH_3 plasma treatment and (**b**) with NH_3 plasma treatment for 3 min. The normalized C-V curve of the $Ce_2Ti_2O_7$ sample (**c**) without NH_3 plasma treatment and (**d**) with NH_3 plasma treatment for 3 min.

shown in Fig. 2(a,b,c and d), XRD patterns reveal that NH_3 plasma treatment for 3 min could drastically enhance the CeO_2 (400) peak and the CeO_2 (200) peak intensity indicative of crystallization during NH_3 plasma treatment. Furthermore, Ti addition could cause CeO_2 crystals to form $Ce_2Ti_2O_7$ crystals as shown in Fig. 3(b). Furthermore, NH_3 plasma treatment for 3 min could enhance crystallization as 3 min NH_3 plasma treatment increased the $Ce_2Ti_2O_7$ (2,2,1) peak and the $Ce_2Ti_2O_7$ (2,1,2) peak drastically. The results show that Ti addition and NH_3 plasma treatment could effectively strengthen crystallization and hence improve the sensing performance of the CeO_2 membrane.

In addition, AFM images as shown in Fig. 4 reveal that the surface roughness of the CeO_2 and $Ce_2Ti_2O_7$ films treated in various NH_3 plasma conditions. Compared with the CeO_2 film and $Ce_2Ti_2O_7$ as shown in Fig. 4, Ti doping could effectively increase the surface roughness and cause the grain on the surface to become more noticeable. Similarly, NH_3 plasma treatment could increase roughness and cause grain growth as well. Moreover, incorporating both Ti doping and NH_3 plasma treatment for 3 min could drastically increase the roughness from 0.424 nm to 0.815 nm and clearly enhance the grains, as shown in the AFM images.

Furthermore, SIMS analysis as shown in Fig. 5 reveals the distribution of various atoms inside the CeO_2/Si film and the $Ce_2Ti_2O_7$/Si films. Figure 5 shows stronger N atom concentrations in both the CeO_2 film and the $Ce_2Ti_2O_7$ film after NH_3 plasma treatment. Moreover, noticeable accumulation could be observed in the membrane/Si interface. Since NH_3 plasma treatment could infuse N atoms into the CeO_2 and $Ce_2Ti_2O_7$ films, stronger N-Ce and N-Si bonds might be formed and dangling bonds or defects around the interface might be fixed[19,23]. Strengthening the material quality in the bulk and in the interface might increase the sensitivity and linearity of pH sensing of the films. Furthermore, a high concentration of Ti atoms in the SIMS profile for the $Ce_2Ti_2O_7$ films could be observed. Since Ti addition could also fix traps and dangling bonds, a high concentration of Ti atoms in the Ti-doped CeO_2 film could cause the Ti atoms to reduce the defects[18]. In addition, a slight increase of concentration of Ti atoms might indicate the accumulation of the Ti atoms around the interface and fix the dangling bonds near the interface.

Incorporating a CeO_2 membrane as the electroactive gate film in the pH-based EIS structure allows the incorporated sensor to detect fine pH value variations. The influence of the plasma treatment and Ti doping can be realized by studying the site binding model[27]. The reference voltage is closely related to the surface potential, which is dependent on the pH value of the electrolyte and the membrane material.

$$\psi = 2.303\frac{kT}{q}\frac{\beta}{\beta+1}(pH_{pzc} - pH) \quad (1)$$

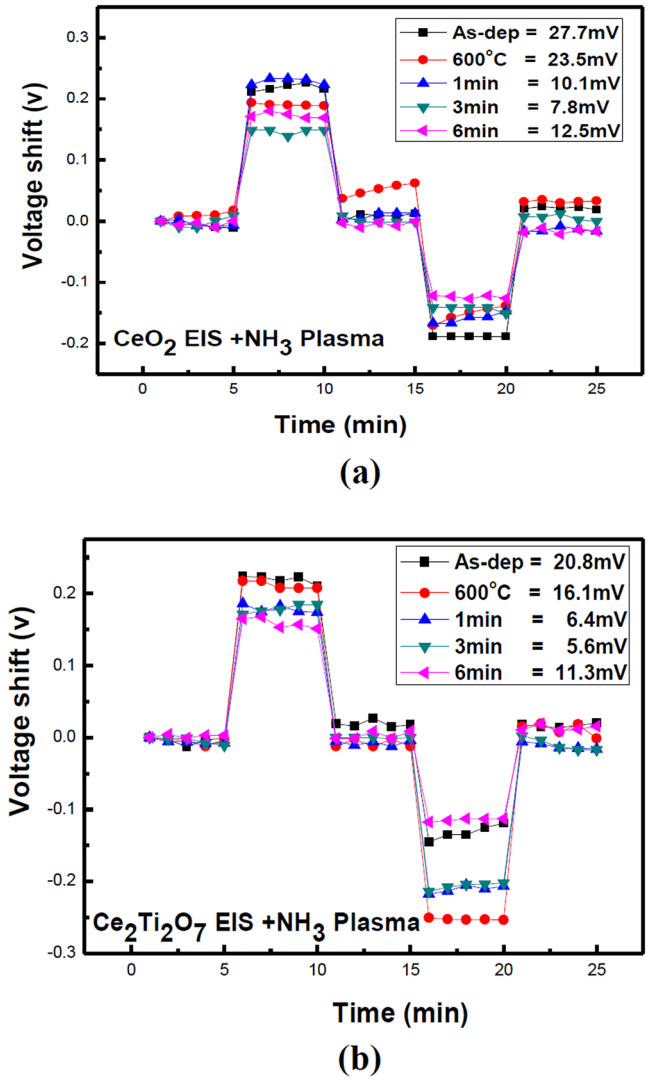

Figure 8. The hysteresis of (**a**) CeO_2 and (**b**) $Ce_2Ti_2O_7$ sensing membrane with NH_3 plasma treatment in various conditions during a pH loop of 7→4→7→10→7 over a period of 25 minutes.

The φ value can be calculated from the above equation (1), where k is the Boltzmann's constant, T is the temperature, and β is a parameter in terms of the chemical sensitivity of the membrane[28–30]. The value of β is proportional to the density of surface hydroxyl groups and is determined by the following equation (2).

$$\beta = \frac{2q^2 Ns\sqrt{K_a K_b}}{KTC_{DL}} \quad (2)$$

N_s is the number of surface sites per unit area. K_a is the equilibrium constant of the acid point and K_b is the equilibrium constant of the base point, respectively. C_{DL} is the bilayer capacitance calculated from the Gouy-Chapman-Stern model[31].

According to the above theories, addition of Ti atoms and incorporation of NH_3 plasma treatment could enhance crystallization and reduce the dangling bonds. Therefore, the number of the surface sites could be increased and the sensing performance could be boosted. To characterize the sensing performance of the CeO_2 and Ce_2TiO_7 membranes with and without NH_3 plasma treatment, the C-V curves of these various membranes are shown in Fig. 6(a,b,c and d). The linearity and sensitivity of the CeO_2 and Ce_2TiO_7 membranes with and without NH_3 plasma treatment extracted from normalized C-V curve are shown in Fig. 7(a,b,c and d). As shown in Fig. 6(a) and 7(a), the as-deposited CeO_2 membrane exhibited a low sensitivity of 34.37 mV/pH. Moreover, fluctuated C-V curves could be observed indicating multi-capacitance effects were present, signifying that defects in the bulk or in the interface might be present. As the membrane underwent the NH_3 plasma treatment for 3 min, the sensitivity was boosted to 48.62 mV/pH and the C-V curves became smoother as shown in Figs 6(b) and 7(b). Similarly, as the as-deposited CeO_2 membrane and the as-deposited Ce_2TiO_7 membrane were compared as shown in Fig. 7(a and c), the sensitivity was improved when the Ti atoms were incorporated into the CeO_2 membrane.

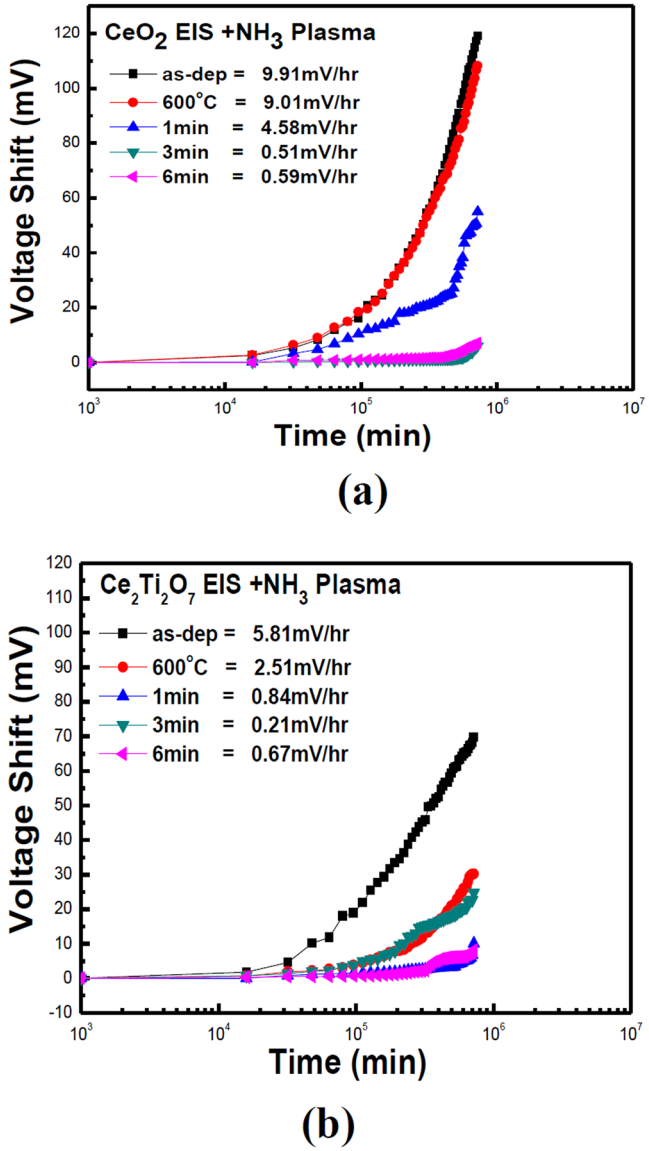

Figure 9. The drift voltage of (**a**) CeO_2 and (**b**) $Ce_2Ti_2O_7$ sensing membrane with NH_3 plasma treatment in various conditions and then dipped in pH7 buffer solution for 12 hours.

Furthermore, as the Ce_2TiO_7 membrane went through NH_3 plasma treatment for 3 min, the sensitivity was greatly improved to 54.43 mV/pH. Furthermore, much smoother C-V curves could be observed, indicating single capacitance with high material quality film could be formed. Combining Ti doping and NH_3 plasma treatment could enhance the CeO_2 film material quality and sensing capability.

Furthermore, to study the hysteresis effects of the CeO_2 and Ce_2TiO_7 films which underwent through various plasma treatment conditions, hysteresis voltages were measured for the CeO_2 film and the $Ce_2Ti_2O_7$ film with different plasma treatment conditions, as shown in Fig. 8(a and b). The as-deposited CeO_2 film with a hysteresis voltage of 27.7 mV and the as-deposited $Ce_2Ti_2O_7$ film with a hysteresis voltage of 20.8 mV could be observed, indicating that Ti-doping might reduce the dangling bonds and traps to lower the hysteresis voltage. Furthermore, the CeO_2 with NH_3 plasma treatment had a low hysteresis voltage of 7.8 mV, and the $Ce_2Ti_2O_7$ film with NH_3 plasma voltage had the lowest hysteresis voltage of 5.6 mV. The results indicate that NH_3 plasma treatment could passivate defects and enhance sensing performance, consistent with the material analysis.

Finally, the CeO_2 membrane and the Ce_2TiO_7 membrane prepared in different plasma treatment conditions were tested for gate drift voltage, as shown in Fig. 9(a and b). Each of the samples were dipped in a pH7 buffer solution. In line with all the previous analyses, results reveal that the drift voltage shift could be reduced either by Ti doping or NH_3 plasma treatment for 3 min. Moreover, the $Ce_2Ti_2O_7$ membrane with NH_3 plasma treatment had the least drift voltage of 0.21 mV/hr, signifying that Ti doping combined with NH_3 plasma treatment could effectively enhance sensing capability. Moreover, to compare EIS membranes composed of various materials and treated with different treatment, the EIS pH biosensing devices incorporating ZnO, Gd_2O_3, Gd_2TiO_7 and Nb_2O_5 membranes are compared with CeO_2 and Ce_2TiO_7 membranes as shown in Table 1 [9,32–34].

Sensing membrane	pH sensitivity (mV/pH)	Hysteresis voltage (mV)	Drift rate (mV/h)
ZnO with RTA	42.54	7.37	1.78
Nb_2O_5 with CF_4	52.15	5.22	3.34
Gd_2O_3 with RTA	48.29	5.8	2.2
Gd_2TiO_7 with RTA	55.27	3.6	1.37
CeO_2	34.37	27.7	9.91
CeO_2 with NH_3	48.62	7.8	0.51
$Ce_2Ti_2O_7$	37.79	20.8	5.81
$Ce_2Ti_2O_7$ with NH_3	52.43	5.6	0.21

Table 1. Comparison with pH sensing devices composed of various membranes with different treatments. (RTA: rapid thermal annealing. CF_4: CF_4 plasma treatment. NH_3: NH_3 plasma treatment).

Conclusions

In this study, CeO_2 EIS biosensors incorporated Ti doping and NH_3 plasma treatment were fabricated. Multiple material analyses suggest that the addition of Ti atoms to form $Ce_2Ti_2O_7$ film could enhance grain growth and suppress dangling bonds. Furthermore, inclusion of N atoms by NH_3 plasma treatment could reinforce crystallization and remove defects. Therefore, the sensitivity and linearity of the CeO_2 EIS biosensor might be boosted and the hysteresis and the drift voltage could be reduced. CeO_2-based EIS membranes with Ti doping and NH_3 plasma treatment show promise for future industrial biosensing applications.

Methods

Electrolyte-insulator-semiconductor (EIS) structures incorporating CeO_2 and $Ce_2Ti_2O_7$ sensing membranes were fabricated on 4 inch n-type (100) silicon wafers with a resistivity of 5–10 Ω-cm. After standard RCA cleaning, the samples were dipped into 1% hydrofluoric acid to etch native oxide from the surface. For the first type of samples, a 50 nm CeO_2 film was deposited on the Si substrate by reactive radio frequency (rf) sputtering from a cerium target in diluted O_2 ambient ($Ar/O_2 = 25$ sccm/0 sccm). For the second group of samples, a 50 nm $Ce_2Ti_2O_7$ sensing film was deposited by reactive radio frequency (rf) co-sputtering on an n-type silicon wafer, sputtered from a cerium target and a titanium target in diluted O_2 ambient ($Ar/O_2 = 20$ sccm/5 sccm). The rf power and chamber pressure were 100 W and 20 mTorr, respectively. After deposition, CeO_2 and $Ce_2Ti_2O_7$ were subjected to a post-NH_3 plasma treatment in a plasma-enhanced chemical vapor deposition (PECVD) system with rf power of 30 W and a processing pressure of 500 mTorr for 1 min, 3 min and 6 min. Next, two types of samples were subsequently treated with rapid thermal annealing (RTA) using a conventional thermal annealing system under ambient N_2 condition for 30 sec at a temperature of 600 °C. After that, the back-side contact of the Si wafer was deposited by Al film with a thickness of 300 nm. The sensing membrane size was defined through photolithographic processing under a photosensitive epoxy (SU8-2005, Micro-Chem). EIS structures were then fabricated on the copper lines of a printed circuit board (PCB) by using a silver gel to form conductive lines. Epoxy was utilized to separate the EIS structure and the copper line. The detailed EIS structure is illustrated in Fig. 1.

References

1. Perley, G. A. An Industrial Salt-Bridge Junction Tube. *Transactions of The Electrochemical Society* **92**, 497, doi:10.1149/1.3071837 (1947).
2. Kittel, H. Industrial pH measurements. *Melliand Textilberichte* **47**, 566 (1966).
3. M. Bacci, F. Baldini, A. Scheggi Chemical studies on acid-base indicators for the development of an extrinsic optical fiber pH sensor, in:OE/Fiber LASE'88, International Society for Optics and Photonics 84 (1989).
4. Li, Y.-J., Wang, Y.-L. & Liu, Q.-Y. The Highly Connected MOFs Constructed from Nonanuclear and Trinuclear Lanthanide-Carboxylate Clusters: Selective Gas Adsorption and Luminescent pH Sensing. *Inorganic Chemistry* **56**, 2159–2164, doi:10.1021/acs.inorgchem.6b02811 (2017).
5. P. Bergveld Development of an ion-sensitive solid state device for neu-rophysiological measurement. *IEEE Trans. Biomed. Eng.* (T-BME) **17**, 70 (1970).
6. F. Tamura, N. Akao, N. Hara, K. Sugimoto Development of EIS capacitor pH sensor for highly corrosive environment, Zairyo-to-Kankyo **46**, 243 (1997).
7. Kukla, A., Kanjuk, N., Starodub, N. & Shirshov, Y. M. Multienzyme electrochemical sensor array for determination of heavy metal ions. *Sensors and Actuators B: Chemical.* **57**, 213–218, doi:10.1016/S0925-4005(99)00153-7 (1999).
8. Schöning, M. J. "Playing around" with field-effect sensors on the basis of EIS structures. *LAPS and ISFETs, Sensors.* **5**, 126 (2005).
9. Kao, C.-H. *et al.* Multi-analyte biosensors on a CF_4 plasma treated Nb_2O_5-based membrane with an extended gate field effect transistor structure. *Sensors and Actuators B: Chemical.* **194**, 419–426, doi:10.1016/j.snb.2013.12.056 (2014).
10. Lu, T.-F. *et al.* Non-ideal effects improvement of SF 6 plasma treated hafnium oxide film based on electrolyte–insulator–semiconductor structure for pH-sensor application. *Microelectronics Reliability.* **50**, 742–746, doi:10.1016/j.microrel.2010.01.029 (2010).
11. Pan, T.-M. & Lin, J.-C. A TiO_2/Er_2O_3 stacked electrolyte/ insulator/ semiconductor film pH-sensor for the detection of urea. *Sensors and Actuators B: Chemical.* **138**, 474–479, doi:10.1016/j.snb.2009.02.063 (2009).
12. de Rouffignac, P., Park, J.-S. & Gordon, R. G. Atomic layer deposition of Y_2O_3 thin films from yttrium tris (N, N′-diisopropylacetamidinate) and water. *Chemistry of materials.* **17**, 4808–4814, doi:10.1021/cm050624+ (2005).
13. Singh, J. & Roychoudhury, A. *et al.* A dual enzyme functionalized nanostructured thulium oxide based interface for biomedical application. *Nanoscale.* **6**, 1195–1208, doi:10.1039/C3NR05043B (2014).
14. Kao, C. H. *et al.* Electrical, material and multianalyte-sensitive characteristics of thermal CeO_2/SiO_2-stacked oxide capacitors. *Thin Solid Films.* **570**, 552–557, doi:10.1016/j.tsf.2014.02.037 (2014).
15. Pan, T.-M., Wang, C.-W. & Pan, S.-Y. High-Performance Electrolyte–Insulator–Semiconductor pH Sensors Using High-CeO_2 Sensing Films. *IEEE Electron Device Letters.* **36**, 1195–1197, doi:10.1109/LED.2015.2475627 (2015).

16. Kao, C. H. *et al*. Effects of N_2 and O_2 annealing on the multianalyte biosensing characteristics of CeO_2-based electrolyte–insulator–semiconductor structures. *Sensors and Actuators B: Chemical.* **194**, 503–510, doi:10.1016/j.snb.2013.12.103 (2014).
17. Kao, C. H. *et al*. Fabrication of multianalyte CeO_2 nanograin electrolyte–insulator–semiconductor biosensors by using CF_4 plasma treatment. *Sensing and Bio-Sensing Research.* **5**, 71–77, doi:10.1016/j.sbsr.2015.07.001 (2015).
18. Kao, C.-H., Chen, H., Chang, H. W. & Chuang, C. S. Electrical and material characterizations of $HfTiO_4$ flash memory devices with post-annealing. *Journal of Vacuum Science & Technology A* **29**, 06B102 (2011).
19. Lai, C.-S. *et al*. Tai. New pH-sensitive $TaO_x N_y$ membranes prepared by NH_3 plasma surface treatment and nitrogen incorporated reactive sputtering. *Sensors and Actuators B: Chemical.* **130**, 77–81, doi:10.1016/j.snb.2007.07.115 (2008).
20. Kim, M.-S. *et al*. Pd–Cu bimetallic catalysts supported on TiO_2–CeO_2 mixed oxides for aqueous nitrate reduction by hydrogen. *Journal of Molecular Catalysis A: Chemical* **392**, 308–314, doi:10.1016/j.molcata.2014.05.034 (2014).
21. Lin, Y.-T. *et al*. Detection of KRAS mutation by combination of polymerase chain reaction (PCR) and EIS sensor with new amino group functionalization. *Sensors and Actuators B: Chemical.* **186**, 374–379, doi:10.1016/j.snb.2013.06.009 (2013).
22. Park, Y. R. & Kim, K. J. Optical and electrical properties of Ti-doped ZnO films: observation of semiconductor–metal transition. *Solid State Communications.* **123**, 147–150, doi:10.1016/S0038-1098(02)00217-X (2002).
23. Wang, F.-S., Tsai, M.-J. & Cheng, H.-C. The effects of NH_3 plasma passivation on polysilicon thin-film transistors. *IEEE Electron Device Letters.* **16**, 503–505, doi:10.1109/55.468281 (1995).
24. Yang, C.-M. *et al*. Low cost and flexible electrodes with NH_3 plasma treatments in extended gate field effect transistors for urea detection. *Sensors and Actuators B: Chemical.* **187**, 274–279, doi:10.1016/j.snb.2012.11.023 (2013).
25. Abe, K., Suzuki, K. & Citterio, D. Inkjet-printed microfluidic multianalyte chemical sensing paper. *Analytical chemistry.* **80**, 6928–6934, doi:10.1021/ac800604v (2008).
26. Hansen, J. A. *et al*. Quantum-dot/aptamer-based ultrasensitive multi-analyte electrochemical biosensor. *Journal of the American Chemical Society.* **128**, 2228–2229, doi:10.1021/ja060005h (2006).
27. Jamasb, S., Collins, S. D. & Smith, R. L. A physical model for threshold voltage instability in Si_3N_4-gate H+-sensitive FET's (pH ISFET's). *IEEE Transactions on Electron Devices.* **45**, 1239–1245, doi:10.1109/16.678525 (1998).
28. Bousse, L., De Rooij, N. & Bergveld, P. Operation of chemically sensitive field-effect sensors as a function of the insulator-electrolyte interface. *IEEE Transactions on Electron Devices.* **30**, 1263–1270, doi:10.1109/T-ED.1983.21284 (1983).
29. Fung, C. D., Cheung, P. W. & Ko, W. H. A generalized theory of an electrolyte-insulator-semiconductor field-effect transistor. *IEEE Transactions on Electron Devices.* **33**, 8–18, doi:10.1109/T-ED.1986.22429 (1986).
30. Van Hal, R., Eijkel, J. & Bergveld, P. A novel description of ISFET sensitivity with the buffer capacity and double-layer capacitance as key parameters. *Sensors and Actuators B: Chemical.* **24**, 201–205, doi:10.1016/0925-4005(95)85043-0 (1995).
31. Oldham, K. B. A Gouy–Chapman–Stern model of the double layer at a (metal)/(ionic liquid) interface. *Journal of Electroanalytical Chemistry.* **613**, 131–138, doi:10.1016/j.jelechem.2007.10.017 (2008).
32. C. H. Kao *et al*. Multianalyte biosensor based on pH-sensitive ZnO electrolyte–insulator–semiconductor structures, Journal of Applied Physics **115**, 184701 (2014).
33. C.H. Kao *et al*. Ti-doped Gd 2 O 3 sensing membrane forelectrolyte–insulator–semiconductor pH sensor, Thin Solid Films **520**, 3760 (2012).
34. J.-J. Wang *et al*. Chen, Electrolyte-Insulator-Semiconductor (EIS) with Gd 2 O 3-based Sensing Membrane for pH-Sensing Applications, Journal of New Materials for Electrochemical Systems **18**, 79 (2015).

Acknowledgements

This work was supported in part by the Ministry of Science and Technology of Taiwan, ROC under Contract No: MOST 104-2221-E-260 -002 -MY3 and MOST 104-2221-E-182-042. Moreover, this work was supported by Chang Gung University under the contract of CMRPD2F0091.

Author Contributions

Chyuan-Haur Kao, Che-Wei Chang, Chan-Yu Lin, and Hsiang Chen designed the research. Che-Wei Chang graphed the device structure. Chia Lung Chang and Hsiang Chen devised the crystal growth method, grew and characterized the materials. Yu Tzu Chen,Wei Ming Su, Chien Cheng Lu analysed the data. and wrote the paper.

Additional Information

Competing Interests: The authors declare that they have no competing interests.

Publisher's note: Springer Nature remains neutral with regard to jurisdictional claims in published maps and institutional affiliations.